Presynaptic spontaneous activity enhances the accuracy of latency coding

Marie Levakova[1]**, Massimiliano Tamborrino**[2]**, Lubomir Kostal**[1]**,**

Petr Lansky[1]

[1]Institute of Physiology of the Czech Academy of Sciences, Videnska 1083, 142 20

Prague 4, Czech Republic.

[2]Institute for Stochastics, Johannes Kepler University Linz, Altenbergerstraße 69, 4040

Linz, Austria.

Keywords: Neural coding, first-spike latency, spontaneous activity, Fisher information,

perfect integrate-and-fire model, Wiener process

Abstract

The time to the first spike after the stimulus onset typically varies with the stimulation

intensity. Experimental evidence suggests that neural systems utilize such response la-

tency to encode information about the stimulus. We investigate the decoding accuracy of the latency code in relation to the level of noise in the form of presynaptic spontaneous activity. Paradoxically, the optimal performance is achieved at a non-zero level of noise and supra-threshold stimulus intensities. We argue that this phenomenon results from from the influence of the spontaneous activity on the stabilization of the membrane potential in the absence of stimulation. The reported decoding accuracy improvement represents a novel manifestation of the noise-aided signal enhancement.

1   Introduction

Rate and temporal coding have been commonly studied in neuroscience to understand how the information about the environment is encoded in neural activity. Rate coding is based on the classical observation by Adrian (1928) that the number of spikes elicited in a certain time window reflects the stimulus intensity, see e.g. Dayan & Abbott (2001); Johnson & Ray (2004); McDonnell & Stocks (2008), whereas in temporal coding spike times are believed to convey important information about the stimulus, cf. Theunissen & Miller (1995); Aihara & Tokuda (2002); Van Rullen et al. (2005); Toyoizumi et al. (2006). The *first-spike latency*, defined as the time from the stimulus onset to the first evoked spike, has been shown to vary with the level of stimulation in several systems, such as auditory (Furukawa & Middlebrooks, 2002; Nelken et al., 2005), visual (Gawne et al., 1996; Reich et al., 2001), olfactory (Rospars et al., 2003) and somatosensory systems (Panzeri et al., 2001; Petersen et al., 2001, 2002). Therefore, latency is investigated as a possible form of temporal code (Jenison, 2001; Gollisch & Meister,

2008; Wainrib et al., 2010; Levakova, 2016). Many statistical methods have been proposed for latency estimation, see e.g. Friedman & Priebe (1998); Baker & Gerstein (2001); Pawlas et al. (2010); Tamborrino et al. (2012, 2013); Levakova et al. (2014) and Levakova et al. (2015) for a review.

Our aim is to understand what are the ultimate limits on the accuracy of stimulus decoding based on the first-spike latency. We employ the Fisher information as classically done in computational neuroscience (Seung & Sompolinsky, 1993; Abbott & Dayan, 1999; Wilke & Eurich, 2002; Johnson & Ray, 2004; Amari & Nakahara, 2005; Lansky & Greenwood, 2005, 2007; Kostal et al., 2015). Since not all stimulus levels can be decoded with the same accuracy, we determine which stimulus intensities can be discriminated most precisely. Furthermore, we investigate how the estimation accuracy depends on the amount of noise in the form of spontaneous activity of presynaptic neurons.

The presence of noise corrupts signal transmission in linear systems. Nevertheless, noise may have a positive effect on signal processing in nonlinear systems, as confirmed by the *stochastic resonance* phenomenon (for a review see McDonnell & Abbott, 2009; McDonnell & Ward, 2011). Stochastic resonance is typically observed in systems with a threshold in presence of a weak signal (Gammaitoni et al., 1998). However, the sub-threshold regime is not a necessary condition when considering more than one neuron, since, for example, a suprathreshold signal may be also enhanced by noise in a network of threshold devices (Stocks, 2000, 2001). Other phenomena where noise enhances the signal are for example *coherence resonance* (Lindner et al., 2002; Kostal et al., 2007) and *firing-rate resonance* (Brunel et al., 2003). In this paper we identify a new kind of a

phenomenon where signal transmission is enhanced by noise. This phenomenon occurs in a setting as simple as the stochastic perfect integrate-and-fire model.

2 Methods

2.1 Neuronal model

Throughout the paper we describe the neuronal activity by means of the perfect integrate-and-fire model introduced by Gerstein & Mandelbrot (1964). The membrane potential dynamics is modeled by a Wiener process $X(t)$, given as the solution to the following stochastic differential equation

$$\mathrm{d}X(t) = \mu \,\mathrm{d}t + \sigma \,\mathrm{d}W(t), \qquad X(0) = 0,$$

where $W(t)$ is a standard (driftless) Wiener process, $\mu > 0$ is the drift and $\sigma > 0$ is the diffusion parameter. The stochastic input to the neuron is accumulated over time without any leakage until $X(t)$ crosses a constant threshold $B > 0$. After that, a spike is elicited, $X(t)$ is reset to its starting value 0 and the accumulation starts anew. The resulting spike train is a renewal point process, where interspike intervals are independent and identically distributed as $IG(B/\mu, B^2/\sigma^2)$, an inverse Gaussian distribution with scale parameter B/μ, shape parameter B^2/σ^2, mean B/μ and variance $B\sigma^2/\mu^3$ (Chhikara & Folks, 1989). The inverse Gaussian distribution has been successfully fitted to interspike interval data of real neurons (Gerstein & Mandelbrot, 1964; Grün & Rotter, 2010, and others). Without loss of generality, the threshold B is set to $B = 1$ throughout the paper.
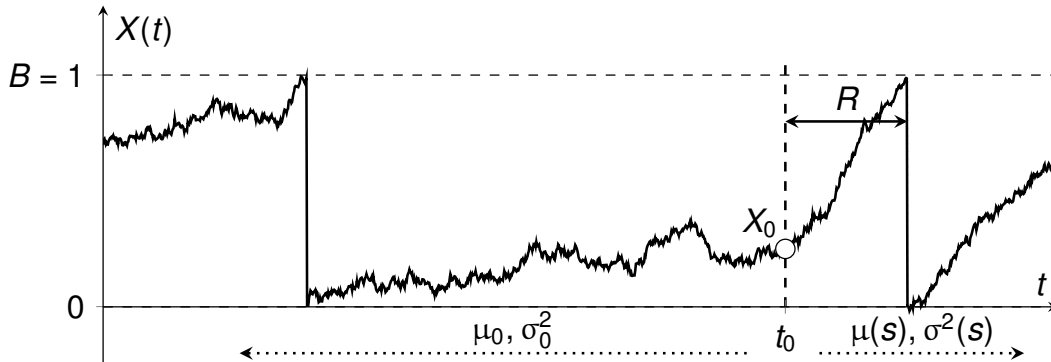
Figure 1: Schematic illustration of the perfect integrate-and-fire model. The graph shows a sample path of the membrane potential $X(t)$. When $X(t)$ exceeds a constant threshold $B = 1$, an action potential is generated. Then $X(t)$ is reset to 0 and its evolution stars anew. At time t_0, a stimulus is applied, and the parameters of the process change from μ_0, σ_0^2 to $\mu(s)$, $\sigma^2(s)$. The time from the stimulus onset to the first evoked spike, called first-spike latency and denoted by R, is used for the estimation of the stimulus intensity s. Finally, X_0 denotes the random position of the membrane potential at time t_0.

The stimulus onset at time t_0 creates a boundary between two different firing regimes, i.e. spontaneous activity (before t_0) and evoked activity (after t_0). Before t_0, the parameters of the Wiener process, which we denote by $\mu = \mu_0$ and $\sigma^2 = \sigma_0^2$, result from spontaneous activity of presynaptic neurons. When a stimulus of intensity s is applied at t_0, the parameters change according to the stimulus level, so that we have $\mu = \mu(s)$ and $\sigma^2 = \sigma^2(s)$. We denote by $R(s)$ the first-spike latency, i.e. the time from the stimulus onset to the first evoked spike, and by X_0 the random position of the membrane potential at time t_0, i.e. $X_0 = X(t_0)$. After $R(s)$, all subsequent interspike intervals are independent and identically distributed as $T(s) \sim IG(B/\mu(s), B^2/\sigma^2(s))$, with mean

$\mathbb{E}[T(s)] = B/\mu(s) = 1/\mu(s)$ and variance $\text{Var}[T(s)] = B\sigma^2(s)/\mu(s)^3 = \sigma^2(s)/\mu(s)^3$.

A schematic description of the neuronal firing activity is presented in Fig. 1.

The Wiener process can be derived as a diffusion approximation of a random walk (Tuckwell, 1988). The membrane potential modeled by a random walk has jumps upon receiving excitatory or inhibitory presynaptic impulses, occurring randomly in time according to a Poisson process with constant rates $\lambda_E > 0$ and $\lambda_I > 0$, respectively. Choosing

$$\mu = a_E\lambda_E - a_I\lambda_I \tag{1}$$

$$\sigma^2 = a_E^2\lambda_E + a_I^2\lambda_I \tag{2}$$

guarantees that the random walk and its diffusion limit, the Wiener process, have the same mean and variance. Here $a_E > 0$ and $a_I > 0$ denote the membrane potential change caused by excitatory and inhibitory impulses, respectively. We set $a_E = a_I = a$ for convenience.

In analogy to Lansky & Sacerdote (2001), we assume the following three scenarios, yielding three possible functional forms for $\sigma^2(s)$:

1. *Constant diffusion parameter*

   The diffusion parameter remains constant before and after stimulation, i.e.

   $$\sigma^2(s) = \sigma_0^2. \tag{3}$$

2. *Proportional diffusion parameter*

   We assume a balanced input (Miura et al., 2007; Sengupta et al., 2013), that is the ratio between the rates of inhibitory and excitatory presynaptic impulses is fixed,

namely $\lambda_I(s)/\lambda_E(s) = c$, for $c > 0$. From (1) and (2), we get

$$\mu(s) = a(1 - c)\lambda_E(s), \tag{4}$$

$$\sigma^2(s) = k\mu(s), \qquad\qquad k = a\frac{1 + c}{1 - c}. \tag{5}$$

3. *Linearly proportional diffusion parameter*

We fix the rate of inhibitory presynaptic impulses, $\lambda_I(s) = c$, and let $\lambda_E(s)$ change. Then (1) and (2) become

$$\mu(s) = a\big[\lambda_E(s) - c\big], \qquad\qquad k = a, \tag{6}$$

$$\sigma^2(s) = k\mu(s) + m, \qquad\qquad m = 2a^2 c. \tag{7}$$

From a formal point of view, the first and the second form of $\sigma^2(s)$ are special cases of the third one.

The probability density function (pdf), mean and variance of the first-spike latency R in the perfect integrate-and-fire model containing a parameter change were derived for different applications (Tamborrino et al., 2015) and are given by

$$
\begin{aligned}
f_R(r; s) = \mu(s) &\left[\Phi\left(\frac{1 - \mu(s)r}{\sigma(s)\sqrt{r}}\right) - \Phi\left(-\frac{\mu(s)\sqrt{r}}{\sigma(s)}\right) \right] + \frac{\mu(s)\sigma_0^2 - 2\mu_0\sigma^2(s)}{\sigma_0^2} \\
&\times \exp\left(\frac{2\mu_0 r\big[\mu_0\sigma^2(s) - \mu(s)\sigma_0^2\big]}{\sigma_0^4}\right) \left[-\Phi\left(-\frac{\big[2\mu_0\sigma^2(s) - \mu(s)\sigma_0^2\big]\sqrt{r}}{\sigma_0^2\sigma(s)}\right)\right. \\
&\left. + \exp\left(\frac{2\mu_0}{\sigma_0^2}\right)\Phi\left(-\frac{2r\mu_0\sigma^2(s) + \big[1 - \mu(s)r\big]\sigma_0^2}{\sigma_0^2\sigma(s)\sqrt{r}}\right)\right]
\end{aligned} \tag{8}
$$

$$\mathbb{E}[R(s)] = \frac{\mu_0 + \sigma_0^2}{2\mu_0\mu(s)}, \tag{9}$$

$$\mathrm{Var}[R(s)] = \frac{\mu_0^2\mu(s) + 6\mu_0^2\sigma^2(s) + 6\mu_0\sigma_0^2\sigma^2(s) + 3\mu(s)\sigma_0^4}{12\mu_0^2\mu^3(s)}, \tag{10}$$

where $\Phi(\cdot)$ denotes the cumulative distribution function of the standard normal distribution.

2.2 Transfer function

The function specifying the relationship between the stimulus and the typical response is called *stimulus-response function* or *transfer function*. In many cases, the stimulus is represented by its intensity x and the response is characterized by the firing rate λ. The transfer function $\lambda(x)$ is commonly described by the Hill function (Frank, 2013)

$$\lambda(x) = \lambda_0 + \frac{Ax^b}{x_0^b + x^b}, \qquad x \geq 0, \tag{11}$$

which was successfully fitted to experimental data (e.g., Chastrette et al., 1998; Nizami, 2002; Rospars et al., 2003; Durant et al., 2007; Grémiaux et al., 2012). Throughout the paper, we use the log transformation of the stimulus intensity, $s = \log x$, for which the transfer function (11) becomes the logistic function

$$\lambda(s) = \lambda_0 + \frac{A}{1 + \mathrm{e}^{-b(s-s_0)}}, \qquad s \in (-\infty, \infty). \tag{12}$$

Here λ_0 is the firing rate of spontaneous activity and if there is no stimulation, that is $s \to -\infty$, then $\lambda(s) \to \lambda_0$. If $s \to \infty$, the firing rate saturates and $\lambda(s) \to \lambda_0 + A$, with A denoting the maximum possible increment in the firing rate. The quantity $b > 0$ controls the steepness of the curve, while $s_0 = \log x_0$ is both the location parameter and the value of s maximizing $\partial_s \lambda(s)$, where ∂_s denotes the derivative with respect to s. The firing rate $\lambda(s)$ is the inverse of the mean interspike interval, $\lambda(s) = 1/\mathbb{E}[T(s)]$. In the perfect integrate-and-fire model with $B = 1$, we have $\mathbb{E}[T(s)] = 1/\mu(s)$, yielding $\mu(s) = \lambda(s)$ and Eq. (12) holds with $\mu_0 = \lambda_0$.

The mean first-spike latency $\mathbb{E}[R(s)]$ depends also on s. Since we study the latency coding, a transfer function linking together stimulus intensity s and mean latency $\mathbb{E}[R(s)]$ is of primary interest. Plugging $\mu(s) = \lambda(s)$ from Eq. (12) with $\lambda_0 = \mu_0$ into

(9) yields the transfer function for the mean first-spike latency in the perfect integrate-and-fire model, namely

$$\mathbb{E}\big[R(s)\big] = \frac{\left(\mu_0 + \sigma_0^2\right)\left(1 + \mathrm{e}^{-b(s-s_0)}\right)}{2\mu_0\left[A + \mu_0\left(1 + \mathrm{e}^{-b(s-s_0)}\right)\right]}. \tag{13}$$

Both $\mu(s)$ and $\mathbb{E}[R(s)]$ are illustrated in Fig. 2.

Intuitively, the best discrimination of the stimulus intensity s can be achieved in the region where the transfer function changes most rapidly, because a change in s would imply a large change in the mean response. Following this idea, the optimal discrimination of the stimulus level is achieved for the value of s maximizing $\partial_s\mathbb{E}[R(s)]$. The maximum slope of $\mathbb{E}[R(s)]$ for the considered model is achieved at

$$s = s_0 - \frac{1}{b}\log\left(1 + \frac{A}{\mu_0}\right). \tag{14}$$

It can be easily shown that if the level of spontaneous activity μ_0 increases while all the other parameters and s are fixed, then the slope of $\mathbb{E}[R(s)]$ decreases. Therefore the accuracy of detecting s deteriorates, if based only on $\mathbb{E}[R(s)]$. This result does not hold only for the logistic transfer function, but for any $\mu(s)$ in the form $\mu(s) = \mu_0 + f(s)$, where f is an increasing function of s, independent of μ_0. As we show in the following, however, the results about decoding accuracy may be different if the variability of observed data is accounted for.

2.3 Fisher information

The optimality criterion based on the maximal slope of the stimulus-response function ignores that the response to the stimulus is stochastic and implicitly assumes that the variability of the response is either absent, or plays no role. In the following we take

into account that the first-spike latency R is a random variable with pdf f_R. A common approach to assess the decoding performance when the response is stochastic is to look at the minimum achievable error when reconstructing, i.e. estimating, the stimulus s from an observation of R. Under some regularity conditions (Pilarski & Pokora, 2015) and for any unbiased estimator $\hat{s}$ of s based on one observation of $R(s)$, the Cramér-Rao inequality holds (Rao, 2002)

$$\text{Var}[\hat{s}] \geq \frac{1}{J(s)}. \tag{15}$$

Here $J(s)$ is the Fisher information that the latency $R(s)$ carries about the stimulus intensity s, and it is given by

$$J(s) = \mathbb{E}\left[(\partial_s \log f_R(r; s))^2\right] = \int_0^\infty \frac{1}{f_R(r; s)} \left[\partial_s f_R(r; s)\right]^2 \, \mathrm{d}r. \tag{16}$$

Therefore the best discrimination of the stimulus intensity is achieved for

$$s^* = \arg \max_{s \in (-\infty, \infty)} J(s), \tag{17}$$

that is for the value s^* minimizing the variance which an unbiased estimator $\hat{s}$ can possibly attain. In general, s^* is different from the value of s maximizing the slope of the transfer function and depends on the response variance, as illustrated in Fig. 2 and shown also by Wilke & Eurich (2002) and Lansky & Greenwood (2007).

If an analytic expression of the Fisher information is not available, we may consider its lower bound $J^{(2)}(s)$ based on the Cauchy-Schwarz inequality (Stemmler, 1996; Greenwood & Lansky, 2005)

$$J^{(2)}(s) = \frac{1}{\text{Var}\left[R(s)\right]} \left(\partial_s \mathbb{E}\left[R(s)\right]\right)^2. \tag{18}$$

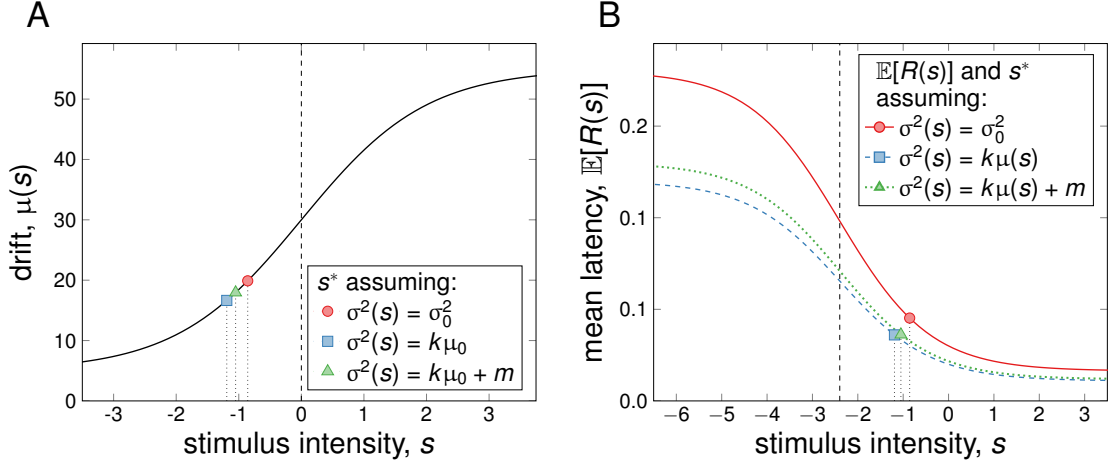We denote by $s^{*(2)}$ the value of s maximizing $J^{(2)}(s)$, which can be considered as an

Figure 2: Transfer functions derived for the perfect integrate-and-fire model and the optimal stimulus intensities maximizing the Fisher information $J(s)$ for different assumptions on the diffusion parameter $\sigma^2(s)$. Panel A: drift $\mu(s)$ given by (12) with $\mu(s) = \lambda(s)$ and $\mu_0 = \lambda_0$; Panel B: mean latency $\mathbb{E}[R(s)]$ given by (13). In both cases, the parameter values are set to $\mu_0 = 5$, $A = 50$, $b = 1$ and $s_0 = 0$. Symbols are used to mark s^* if: $\sigma^2(s) = \sigma_0^2 = 4$ (red circles); $\sigma^2(s) = k\mu(s)$, with $k = 0.2$ (blue squares); $\sigma^2(s) = k\mu(s) + m$, with $k = 0.1$ and $m = 1$ (green triangles). The dashed vertical lines mark the stimulus levels s maximizing the slope of the corresponding transfer functions, i.e. $\partial_s\mu(s)$ and $\partial_s\mathbb{E}[R(s)]$, respectively, which are different from s^*.

approximation of s^* when the Fisher information does not differ too much from its lower bound.

3 Results

An analytical expression of the Fisher information $J(s)$ for the signal intensity s in the perfect integrate-and-fire model is not available in a closed form and must be numeri-

Table 1: Properties of the Fisher information about s for the three considered scenarios.

	Scenario		
	$\sigma^2(s) = \sigma_0^2$	$\sigma^2(s) = k\mu(s)$	$\sigma^2(s) = k\mu(s) + m$
$J(s)$ wrt μ_0	maximum for $\mu_0 > 0$	decreasing in μ_0	maximum for $\mu_0 > 0$
$J(s)$ wrt other parameters	decreasing in σ_0^2	decreasing in k	decreasing in k decreasing in m
$s^{*(2)}$	not available in a closed form	$s_0 - \frac{1}{2b} \log \left(1 + \frac{A}{\mu_0} \right)$	not available in a closed form

cally computed. The lower bound $J^{(2)}(s)$ is equal to

$$J^{(2)}(s) = \frac{[\partial_s \mu(s)]^2}{\mu(s)} \frac{3(\mu_0 + \sigma_0^2)^2}{\mu_0^2 \mu(s) + 6\mu_0 \sigma^2(s)(\mu_0 + \sigma_0^2) + 3\mu(s)\sigma_0^4}.$$

The behavior of the Fisher information in the three studied scenarios is illustrated in Fig. 3 and the key findings are summarized in Table 1.

The behavior of $J(s)$ with respect to s is similar in all the three scenarios. When $\mu_0 > 0$, $J(s)$ starts from 0 as $s \to -\infty$, reaches its maximum at s^* and decreases back to zero as $s \to \infty$. Neither s^* nor $s^{*(2)}$ can be analytically computed, except for $s^{*(2)}$ for the second scenario (see Table 1).

Consider now $J(s)$ for fixed s and allow the spontaneous drift μ_0 to vary. As illustrated in Fig. 3, $J(s)$ is not always decreasing with respect to μ_0 in the first and the third scenario, as one would intuitively expect. On the contrary, we observe a maxi-

mum of the Fisher information at a non-zero value of μ_0, as long as s is not too weak. Therefore, a certain positive level of background activity can enhance the estimation accuracy of s. That is, increasing the amount of spontaneous activity up to some optimal value $\mu_0 = \mu_0^*$ allows a better estimation of s. This phenomenon represents a novel manifestation of a noise-induced signal enhancement. The optimal level μ_0^* is approximately zero for weak stimuli, increases with increasing s and gradually saturates, as observed in Fig. 3 (A, E). A heuristic explanation of the sigmoidal shape of $\mu_0^*(s)$ is that μ_0^* must keep a certain proportion to $\mu(s)$. Differently from what is observed in the first and the third scenario, $J(s)$ is always decreasing in μ_0 in the second scenario, i.e. $\sigma^2(s) = k\mu(s)$, as illustrated in Fig. 3 (C, D). Hence, the presence of the spontaneous drift μ_0 deteriorates the estimation accuracy of s and no noise-induced signal enhancement is possible.

Finally, if both s and μ_0 are fixed, it can be shown that the Fisher information is always decreasing with respect to the parameters affecting the diffusion coefficient, that is σ_0^2, k and (k, m) in the first, second and third scenario, respectively (results not shown).

Reasons why the Fisher information about s is nondecreasing in μ_0   We saw that $J(s)$ is not decreasing in μ_0 if the stimulus intensity s is large enough and if either $\sigma^2(s) = \sigma_0^2$ or $\sigma^2(s) = k\mu(s) + m$. The reason for this noise-induced signal enhancement lies in the influence that μ_0 has on the distribution of $X_0 = X(t_0)$, the random position of the membrane potential at the time of stimulus onset. On one hand, μ_0 determines the trajectory of $X(t)$ before t_0, affecting the distribution of X_0. On the other

hand, if $X_0 = x_0$ is given, μ_0 influences the speed with which $X(t)$ approaches the threshold. Indeed, the conditional distribution of $R(s)$ given that $X_0 = x_0$, denoted by $R(s)|X_0$, is inverse Gaussian with mean $\mathbb{E}[R(s)|X_0] = (B - x_0)/\mu(s)$ and variance $\mathrm{Var}\,[R(s)|X_0] = (B - x_0)\sigma^2(s)/\mu^3(s)$ (with $B = 1$ throughout the paper). Thus $R(s)|X_0$ depends on μ_0 through $\mu(s)$. In the following we study the influence of μ_0 on $R(s)|X_0$ and X_0 separately, and provide heuristic explanation of the positive effect of spontaneous activity on stimulus estimation.

If $\sigma^2(s) = k\mu(s) + m$, the Fisher information about s based on $R(s)|X_0$ and its lower bound, denoted by $J_{s|x_0}(s)$ and $J_{s|x_0}^{(2)}(s)$, respectively, are given by

$$
\begin{aligned}
J_{s|x_0}(s) &= \frac{[\partial_s\mu(s)]^2}{\mu(s)} \frac{k^2\mu(s) + 2(1 - x_0)\,[k\mu(s) + m]}{2\,[k\mu(s) + m]^2}, \\
J_{s|x_0}^{(2)}(s) &= \frac{[\partial_s\mu(s)]^2}{\mu(s)} \frac{(1 - x_0)}{k\mu(s) + m}.
\end{aligned}
\tag{19}
$$

The values for the first and the second scenario can be easily calculated choosing $k = 0$ and $m = 0$, respectively. For any transfer function for the drift in the form $\mu(s) = \mu_0 + f(s)$, e.g. the considered logistic transfer function, and for any choice of k and m, the derivative of $J_{s|x_0}(s)$ with respect to μ_0 is negative and thus $J_{s|x_0}(s)$ is decreasing in μ_0. Hence, if the noise-induced signal enhancement is present, it has to be caused by the influence of μ_0 on X_0.

The pdf, mean and variance of X_0 are given by (Tamborrino et al., 2015)

$$
f_{X_0}(x) = \mathrm{e}^{\alpha(x - |x|)} - \mathrm{e}^{2\alpha(x - 1)},
\tag{20}
$$

$$
\mathbb{E}[X_0] = \frac{1}{2} - \frac{1}{2\alpha}, \qquad \mathrm{Var}[X_0] = \frac{1}{12} + \frac{1}{4\alpha^2},
\tag{21}
$$

where the original parameters μ_0 and σ_0^2 are replaced by a single parameter $\alpha = \mu_0/\sigma_0^2$. In the first and third scenario, α increases when μ_0 increases. Indeed, the diffusion

14

parameter σ_0^2 is either fixed or grows slower than μ_0. Therefore, $\mathbb{E}[X_0]$ and $\text{Var}(X_0)$ become closer to $1/2$ and $1/12$, respectively, implying that the membrane potential is less likely to become negative and it is more centered around its mean value. In the second scenario, i.e. $\sigma_0^2 = k\mu_0$, $\alpha = 1/k$ and thus the distribution of X_0 does not depend on μ_0.

To better understand the influence of μ_0 on X_0, we calculate the differential entropy $h(X_0)$ of X_0, which can be interpreted as a measure of the randomness of X_0. The higher is $h(X_0)$, the more random is X_0. After some calculations, we get

$$h(X_0) = - \int_{-\infty}^{1} f_{X_0}(x) \log f_{X_0}(x) \, \mathrm{d}x = \frac{\pi^2 - 6\text{Li}_2\left(e^{-2\alpha}\right)}{12\alpha}, \qquad (22)$$

where $\text{Li}_2(x)$ denotes the dilogarithm function, $\text{Li}_2(x) = \int_x^0 \log(1-t)/t \, \mathrm{d}t$. It can be shown that $h(X_0)$ is decreasing in α, and thus in μ_0, for fixed σ_0^2. As also illustrated in Fig. 4, when μ_0 and thus α increase, the differential entropy $h(X_0)$ decreases and the pdf of X_0 is more peaked, suggesting a better predictability of the starting position X_0. The dependence of α, $\mathbb{E}[X_0]$, $\text{Var}[X_0]$ and $h(X_0)$ on μ_0 under the three considered scenarios is summarized in Table 2.

If $\sigma_0^2 = k\mu_0$, then $\alpha = 1/k$ and neither f_{X_0} nor $h(X_0)$ depend on μ_0. Moreover, we saw that $J_{s|x_0}(s)$ is decreasing in μ_0 and therefore it is not surprising that also $J(s)$ is decreasing in μ_0. In the other two scenarios, however, f_{X_0} and $h(X_0)$ do depend on μ_0 through α. If we suppress the neuron by letting $\mu_0 \to 0$, then f_{X_0} becomes flat, $\mathbb{E}[X_0] \to -\infty$, $\text{Var}[X_0] \to \infty$ and $h(X_0) \to \infty$. In this case then, the initial position X_0 is extremely uncertain. Thus an increase in μ_0 reduces $h(X_0)$ and makes X_0 more predictable. Combining the influence of μ_0 on X_0 and $R|X_0$, we see that the presence of spontaneous activity $\mu_0 > 0$ deteriorates the inference about s through $R(s)|X_0$, but

15

Table 2: Distribution of X_0 in the three studied scenarios. Here Li_2 denotes the dilogarithm function $\mathrm{Li}_2(x) = \int_x^0 \log(1-t)/t\,\mathrm{d}t$.

	Scenario		
	$\sigma_0^2 = \text{const.}$	$\sigma_0^2 = k\mu_0$	$\sigma_0^2 = k\mu_0 + m$
$\alpha = \mu_0/\sigma_0^2$	μ_0/σ_0^2	$1/k$	$\mu_0/(k\mu_0 + m)$
$h(X_0)$	decreasing in μ_0	constant	decreasing in μ_0
$\lim\limits_{\mu_0 \to 0} \mathbb{E}[X_0]$	$-\infty$	$(1-k)/2$	$-\infty$
$\lim\limits_{\mu_0 \to 0} \mathrm{Var}[X_0]$	∞	$(1+3k^2)/12$	∞
$\lim\limits_{\mu_0 \to \infty} h(X_0)$	0	$\frac{k}{12}\left[\pi^2 - 6\mathrm{Li}_2\left(\mathrm{e}^{-\frac{2}{k}}\right)\right]$	0
$\lim\limits_{\mu_0 \to \infty} \mathbb{E}[X_0]$	$1/2$	$(1-k)/2$	$(1-k)/2$
$\lim\limits_{\mu_0 \to \infty} \mathrm{Var}[X_0]$	$1/2$	$(1+3k^2)/12$	$(1+3k^2)/12$
$\lim\limits_{\mu_0 \to 0} h(X_0)$	∞	$\frac{k}{12}\left[\pi^2 - 6\mathrm{Li}_2\left(\mathrm{e}^{-\frac{2}{k}}\right)\right]$	∞

improves the predictability of the starting position X_0, as long as the distribution of X_0 does depend on μ_0, i.e., $\sigma_0^2 \neq k\mu_0$. For suitable values of μ_0, the positive influence of μ_0 on the distribution of X_0 is stronger than the negative effect on $J_{s|x_0}(s)$, implying the observed increasing behavior of the Fisher information about s with respect to μ_0.

4 Discussion

The finding that spontaneous activity may enhance the signal in a model as simple as the perfect integrate-and-fire is noteworthy, since positive effects of noise on signal transmission are commonly observed in more complicated models. Also the nature of noise-induced signal enhancement reported here is not typical, since it does not result from a subthreshold signal, which is a characteristic feature of stochastic resonance. Although the model contains a threshold B, it does not constitute a barrier for weak signals, but affects only the timing of the discharge.

The key factor causing the signal enhancement in our setting is the noise-induced stabilization of the membrane potential in the stimulation-free regime. By stabilization we mean that the variability of the membrane potential is reduced and excursions of the membrane potential into negative values become unlikely. As we have shown, the role of spontaneous activity on stimulus decoding is interconnected with the effect of spontaneous activity on the randomness of X_0, as indicated by its differential entropy. In particular, the differential entropy of X_0 may approach ∞ for $\mu_0 \to 0$. Thus, the stabilization of X_0 induced by a small increase in μ_0 is substantial and can outweigh the change in $J_{s|x_0}(s)$, which is always decreasing in μ_0. For this reason, we presume that a necessary condition for enhancing the signal by the spontaneous activity is that the uncertainty about X_0 decreases with increasing μ_0. This happens if and only if $\alpha = \mu_0/\sigma_0^2 \to 0$ as $\mu_0 \to 0$, which is the reason why no noise-induced signal enhancement is observed for $\sigma_0^2 = k\mu_0$.

Here we considered and studied only the effect of a step function stimulus, neglecting the end of the stimulation. Of course, a stimulation can have a different form, for

example a pulse. Although the distribution of R would be somewhat different, our analysis could be done analogously. Obviously, the membrane potential X_0 at the stimulus onset would depend on μ_0 in exactly the same way as in the case studied here, so the signal enhancing effect of spontaneous activity might be possibly found also there. Nevertheless, a detailed study is out of the scope of this paper.

The possibility of obtaining infinite differential entropy of X_0 is due to the fact that the perfect integrate-and-fire model has no limitation on the minimum of $X(t)$. If we consider a more realistic neuronal model, such as one of the leaky integrate-and-fire models, the leakage pushes automatically the membrane potential to a resting level, and thus an extreme depolarization of the neuron is less likely to happen. For this type of models, we speculate that both spontaneous activity μ_0 and membrane time constant τ stabilize the membrane potential X_0 and thus may enhance the stimulus detection. However, we must bear in mind that the membrane time constant τ is determined by the biophysical properties of the neuron, while the spontaneous activity μ_0 has less biological restrictions. Consequently, the sensitivity of the neuron to specific stimuli may be adjusted by changes in the activity of presynaptic neurons. The analysis of the leaky integrate-and-fire model is not provided here, because none of the pdfs of the involved quantities of interest are known in a closed form and thus a different approach based on numerical evaluations must be employed. Note that the perfect integrate-and-fire model is a limit case of the leaky integrate-and-fire model for $\tau \to \infty$.

Although the calculations are done for a specific transfer function, our choice of the Hill function is inconsequential for the main result of the paper, which is more general. The phenomenon of noise-induced signal enhancement can be observed for any transfer

function in the form $\mu(s) = \mu_0 + f(s)$, where f is independent of μ_0. As pointed out by Kostal & Lansky (2015), the choice of the stimulus scale is also an integral part of the neural coding problem and may have a significant influence on the estimation accuracy. For this reason, we assume s to be expressed in units on a physiologically relevant scale.

The essential assumption in our approach is that the time t_0 of the stimulus onset is known, which requires a nervous system to maintain a temporal reference about the stimulus onset. An example of such a reference can be a saccadic eye movement (Gerstner & Kistler, 2002) and other possible ways were outlined by Panzeri et al. (2014). If the stimulus onset is completely unknown and can be neither determined nor approximated, the provided Fisher information may be considered as an upper bound for the Fisher information corresponding to a situation when the knowledge of t_0 is not reflected in the first-spike data available for estimation.

It is tempting to speculate that the described enhacement of coding precision due to presynaptic spontaneous activity occurs in the natural sensory information processing. For example, the moth pheromone reception system is organized so that many sensory neurons in the first layer converge onto a small number of output neurons in the second layer (Hansson, 1995). There is an indirect evidence for mechanisms that adjust the level of presynaptic spontaneous activity (as pooled from the sensory neurons), received by the output neurons (Rospars et al., 2014). We hypothesize that the resulting stabilization of the output neuron membrane potential contributes to the high coding precision of the stimulus intensity, which cannot be explained by the convergence layout alone (Rospars et al., 2014).

5 Conclusions

We have shown that the presence of presynaptic spontaneous activity may improve the decoding of the stimulus intensity in a model of a single neuron as simple as the perfect integrate-and-fire model. A key role in determining whether the spontaneous activity can improve the estimation of the stimulus level is played by the distribution of the membrane potential at time of the stimulus onset. A necessary condition is that the randomness in X_0, captured for example by the differential entropy, decreases when the spontaneous activity increases.

Acknowledgments

References

Abbott, L., & Dayan, P. (1999). The effect of correlated variability on the accuracy of a population code. *Neural Comput.*, *11*(1), 91–101.

Adrian, E. D. (1928). *The basis of sensation*. WW Norton & Co.

Aihara, K., & Tokuda, I. (2002). Possible neural coding with interevent intervals of synchronous firing. *Phys. Rev. E*, *66*(2), 026212.

Amari, S., & Nakahara, H. (2005). Difficulty of singularity in population coding. *Neural Comput.*, *17*(4), 839–858.

Baker, S. N., & Gerstein, G. L. (2001). Determination of response latency and its application to normalization of cross-correlation measures. *Neural Comput.*, *13*, 1351–1377.

Brunel, N., Hakim, V., & Richardson, M. J. (2003). Firing-rate resonance in a generalized integrate-and-fire neuron with subthreshold resonance. *Phys. Rev. E*, *67*(5), 051916.

Chastrette, M., Thomas-Danguin, T., & Rallet, E. (1998). Modelling the human olfactory stimulus-response function. *Chem Senses*, *23*, 181–196.

Chhikara, R. S., & Folks, J. L. (1989). *The inverse Gaussian distribution: theory, methodology, and applications*. Marcel Dekker, New York.

Dayan, P., & Abbott, L. F. (2001). *Theoretical neuroscience*. MIT Press.

Durant, S., Clifford, C. W. G., Crowder, N. A., Price, N. S. C., & Ibbotson, M. R. (2007). Characterizing contrast adaptation in a population of cat primary visual cortical neurons using fisher information. *J Opt. Soc. Am. A*, *24*, 1529–1537.

Frank, S. A. (2013). Input-output relations in biological systems: measurement, informatiom and the hill equation. *Biology Direct*, *8*, 31.

Friedman, H. S., & Priebe, C. E. (1998). Estimating stimulus response latency. *J Neurosci Methods*, *83*, 185–194.

Furukawa, S., & Middlebrooks, J. C. (2002). Cortical representation of auditory space: information-bearing features of spike patterns. *J. Neurophysiol.*, *87*(4), 1749–1762.

Gammaitoni, L., Hänggi, P., Jung, P., & Marchesoni, F. (1998). Stochastic resonance. *Reviews of Modern Physics*, *70*(1), 223–287.

Gawne, T. J., Kjaer, T. W., & Richmond, B. J. (1996). Latency: another potential code for feature binding in striate cortex. *J. Neurophysiol.*, *76*(2), 1356–1360.

Gerstein, G., & Mandelbrot, B. (1964). Random walk models for the spike activity of a single neuron. *Biophys. J.*, *4*, 41–68.

Gerstner, W., & Kistler, W. M. (2002). *Spiking Neuron Models*. Cambridge University Press.

Gollisch, T., & Meister, M. (2008). Rapid neural coding in the retina with relative spike latencies. *Science*, *319*(5866), 1108–1111.

Greenwood, P. E., & Lansky, P. (2005). Optimum signal in a simple neuronal model with signal-dependent noise. *Biol. Cybern.*, *92*(3), 199–205.

Grémiaux, A., Nowotny, T., Martinez, D., Lucas, P., & Rospars, J.-P. (2012). Modelling the signal delivered by a population of first-order neurons in a moth olfactory system. *Brain Res.*, *1434*, 123–135.

Grün, S., & Rotter, S. (2010). *Analysis of parallel spike trains*. New York: Springer, first ed.

Hansson, B. (1995). Olfaction in lepidoptera. *Experientia*, *51*(11), 1003–1027.

Jenison, R. L. (2001). Decoding first-spike latency: a likelihood approach. *Neurocomputing*, *38*, 239–248.

Johnson, D. H., & Ray, W. (2004). Optimal stimulus coding by neural populations using rate codes. *J Comput Neurosci*, *16*(2), 129–138.

Kostal, L., & Lansky, P. (2015). Coding accuracy is not fully determined by the neuronal model. *Neural Comput.*, *27*, 1051–1057.

Kostal, L., Lansky, P., & Pilarski, S. (2015). Performance breakdown in optimal stimulus decoding. *J. Neural Eng.*, *12*(3), 036012.

Kostal, L., Lansky, P., & Zucca, C. (2007). Randomness and variability of the neuronal activity described by the Ornstein-Uhlenbeck model. *Netw. Comput. Neural Syst.*, *18*, 63–75.

Lansky, P., & Greenwood, P. E. (2005). Optimal signal estimation in neuronal models. *Neural Comput.*, *17*(10), 2240–2257.

Lansky, P., & Greenwood, P. E. (2007). Optimal signal in sensory neurons under an extended rate coding concept. *BioSystems*, *89*(1), 10–15.

Lansky, P., & Sacerdote, L. (2001). The Ornstein-Uhlenbeck neuronal model with signal-dependent noise. *Physics Letters A*, *285*, 132–140.

Levakova, M. (2016). Effect of spontaneous activity on stimulus detection in a simple neuronal model. *Math. Biosci. Eng.*, *13*, 551–568.

Levakova, M., Ditlevsen, S., & Lansky, P. (2014). Estimating latency from inhibitory input. *Biol. Cybern.*, *108*, 475–493.

Levakova, M., Tamborrino, M., Ditlevsen, S., & Lansky, P. (2015). A review of the methods for neuronal response latency estimation. *BioSystems*, *136*, 23–34.

Lindner, B., Schimansky-Geier, L., & Longtin, A. (2002). Maximizing spike train coherence or incoherence in the leaky integrate-and-fire model. *Phys. Rev. E*, *66*(3), 031916.

McDonnell, M. D., & Abbott, D. (2009). What is stochastic resonance? Definitions, misconceptions, debates and its relevance to biology. *PLoS Comput. Biol.*, *5*(5), e1000348.

McDonnell, M. D., & Stocks, N. G. (2008). Maximally informative stimuli and tuning curves for sigmoidal rate-coding neurons and populations. *Phys. Rev. Lett.*, *101*(5), 058103.

McDonnell, M. D., & Ward, L. M. (2011). The benefits of noise in neural systems: bridging theory and experiment. *Nature Reviews Neuroscience*, *12*(7), 415–426.

Miura, K., Tsubo, Y., Okada, M., & Fukai, T. (2007). Balanced excitatory and inhibitory inputs to cortical neurons decouple firing irregularity from rate modulations. *J. Neurosci.*, *27*(50), 13802–13812.

Nelken, I., Chechik, G., Mrsic-Flogel, T. D., King, A. J., & Schnupp, J. W. (2005). Encoding stimulus information by spike numbers and mean response time in primary auditory cortex. *J. Comput. Neurosci.*, *19*(2), 199–221.

Nizami, L. (2002). Estimating auditory neuronal dynamic range using a fitted function. *Hearing Res.*, *167*(1), 13–27.

Panzeri, S., Ince, R. A., Diamond, M. E., & Kayser, C. (2014). Reading spike timing

without a clock: intrinsic decoding of spike trains. *Phil. Trans. R. Soc. B*, *369*(1637), 20120467.

Panzeri, S., Petersen, R. S., Schultz, S. R., Lebedev, M., & Diamond, M. E. (2001). The role of spike timing in the coding of stimulus location in rat somatosensory cortex. *Neuron*, *29*(3), 769–777.

Pawlas, Z., Klebanov, L. B., Beneš, V., Prokešová, M., Popelář, J., & Lansky, P. (2010). First-spike latency in the presence of spontaneous activity. *Neural Comput.*, *22*(7), 1675–1697.

Petersen, R. S., Panzeri, S., & Diamond, M. E. (2001). Population coding of stimulus location in rat somatosensory cortex. *Neuron*, *32*(3), 503–514.

Petersen, R. S., Panzeri, S., & Diamond, M. E. (2002). The role of individual spikes and spike patterns in population coding of stimulus location in rat somatosensory cortex. *BioSystems*, *67*(1), 187–193.

Pilarski, S., & Pokora, O. (2015). On the Cramér-Rao bound applicability and the role of Fisher information in computational neuroscience. *BioSystems*, *136*, 11–22.

Rao, C. R. (2002). *Linear Statistical Inference and Its Applications*. New York: John Wiley & Sons, 2nd ed.

Reich, D. S., Mechler, F., & Victor, J. D. (2001). Temporal coding of contrast in primary visual cortex: when, what, and why. *J. Neurophysiol.*, *85*(3), 1039–1050.

Rospars, J.-P., Grémiaux, A., Jarriault, D., Chaffiol, A., Monsempes, C., Deisig, N., Anton, S., Lucas, P., & Martinez, D. (2014). Heterogeneity and convergence of

olfactory first-order neurons account for the high speed and sensitivity of second-order neurons. *PLoS Comput Biol*, *10*(12), e1003975.

Rospars, J.-P., Lansky, P., Duchamp, A., & Duchamp-Viret, P. (2003). Relation between stimulus and response in frog olfactory receptor neurons in vivo. *Eur. J. Neurosci.*, *18*(5), 1135–1154.

Sengupta, B., Laughlin, S. B., & Niven, J. E. (2013). Balanced excitatory and inhibitory synaptic currents promote efficient coding and metabolic efficiency. *PLoS Comput. Biol.*, *9*(5), e1003263.

Seung, H. S., & Sompolinsky, H. (1993). Simple models for reading neuronal population codes. *Proc. Natl. Acad. Sci. USA*, *90*(22), 10749–10753.

Stemmler, M. (1996). A single spike suffices: the simplest form of stochastic resonance in model neurons. *Network*, *7*(4), 687–716.

Stocks, N. (2000). Suprathreshold stochastic resonance in multilevel threshold systems. *Phys. Rev. Lett.*, *84*(11), 2310–2313.

Stocks, N. (2001). Information transmission in parallel threshold arrays: Suprathreshold stochastic resonance. *Phys. Rev. E*, *63*(4), 041114.

Tamborrino, M., Ditlevsen, S., & Lansky, P. (2012). Identification of noisy response latency. *Phys. Rev. E*, *86*, 021128.

Tamborrino, M., Ditlevsen, S., & Lansky, P. (2013). Parametric inference of neuronal response latency in presence of a background signal. *BioSystems*, *112*(3), 249–257.

Tamborrino, M., Ditlevsen, S., & Lansky, P. (2015). Parameter inference from hitting times for perturbed Brownian motion. *Lifetime Data Anal.*, *21*(3), 331–352.

Theunissen, F., & Miller, J. P. (1995). Temporal encoding in nervous systems: a rigorous definition. *J. Comput. Neurosci.*, *2*(2), 149–162.

Toyoizumi, T., Aihara, K., & Amari, S. (2006). Fisher information for spike-based population decoding. *Phys. Rev. Lett.*, *97*(9), 098102.

Tuckwell, H. C. (1988). *Introduction to Theoretical Neurobiology, Vol.2: Nonlinear and Stochastic Theories*. Cambridge Univ. Press, Cambridge.

Van Rullen, R., Guyonneau, R., & Thorpe, S. (2005). Spike times make sense. *Trends Neurosci.*, *28*, 1–4.

Wainrib, G., Thieullen, M., & Pakdaman, K. (2010). Intrinsic variability of latency to first-spike. *Biol. Cybern.*, *103*, 43–56.

Wilke, S. D., & Eurich, C. W. (2002). Representational accuracy of stochastic neural populations. *Neural Comput.*, *14*(1), 155–189.

1st scenario: $\sigma^2(s) = \sigma_0^2$

A

B

2nd scenario: $\sigma^2(s) = k\mu(s)$

C

D

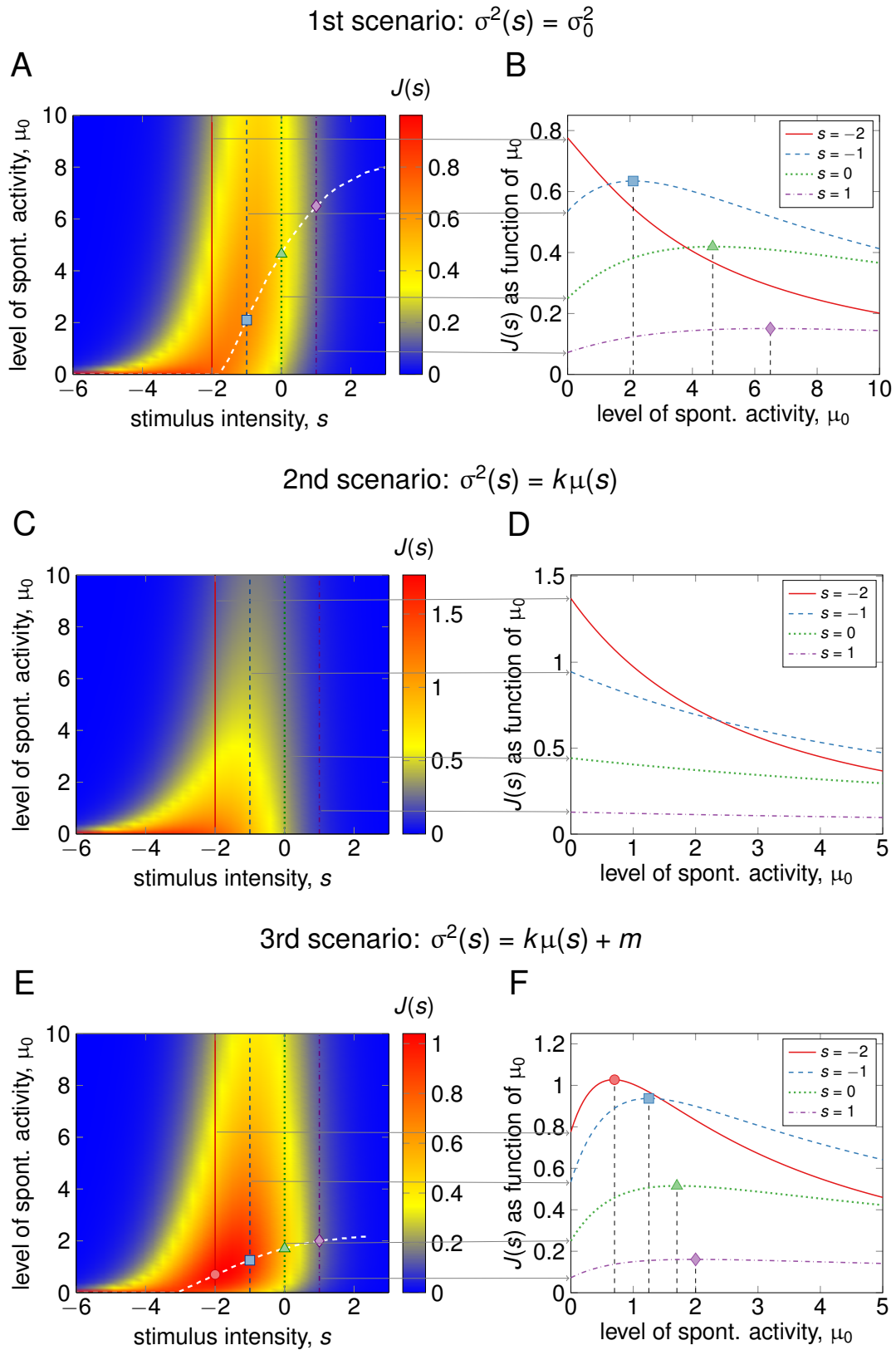3rd scenario: $\sigma^2(s) = k\mu(s) + m$

E

F

Figure 3: Caption on the next page.

Figure 3: (Previous page.) Fisher information $J(s)$ about the stimulus intensity s for the perfect integrate-and-fire model. The results in the first and the third row reveal that the Fisher information about s is not always decreasing when the level of noise μ_0 increases. Left column: Dependence of $J(s)$ on s and μ_0, with values of $J(s)$ given by colors. Vertical lines: values of s for which $J(s)$ is drawn in the right column. The dashed white line corresponds to the value of spontaneous activity $\mu_0 = \mu_0^*$ maximizing $J(s)$ for a given s. Right column: Dependence of $J(s)$ on μ_0 for selected values of s (marked by vertical lines in the left column). The Fisher information is computed for the same three scenarios and parameter values as in Fig. 2: $\sigma^2(s) = \sigma_0^2 = 4$ (Panels A, B); $\sigma^2(s) = k\mu(s)$, with $k = 0.2$ (Panels C, D); $\sigma^2(s) = k\mu(s) + m$, with $k = 0.1$ and $m = 1$ (Panels E, F). Values of the other parameters are $A = 50$, $b = 1$ and $s_0 = 0$.
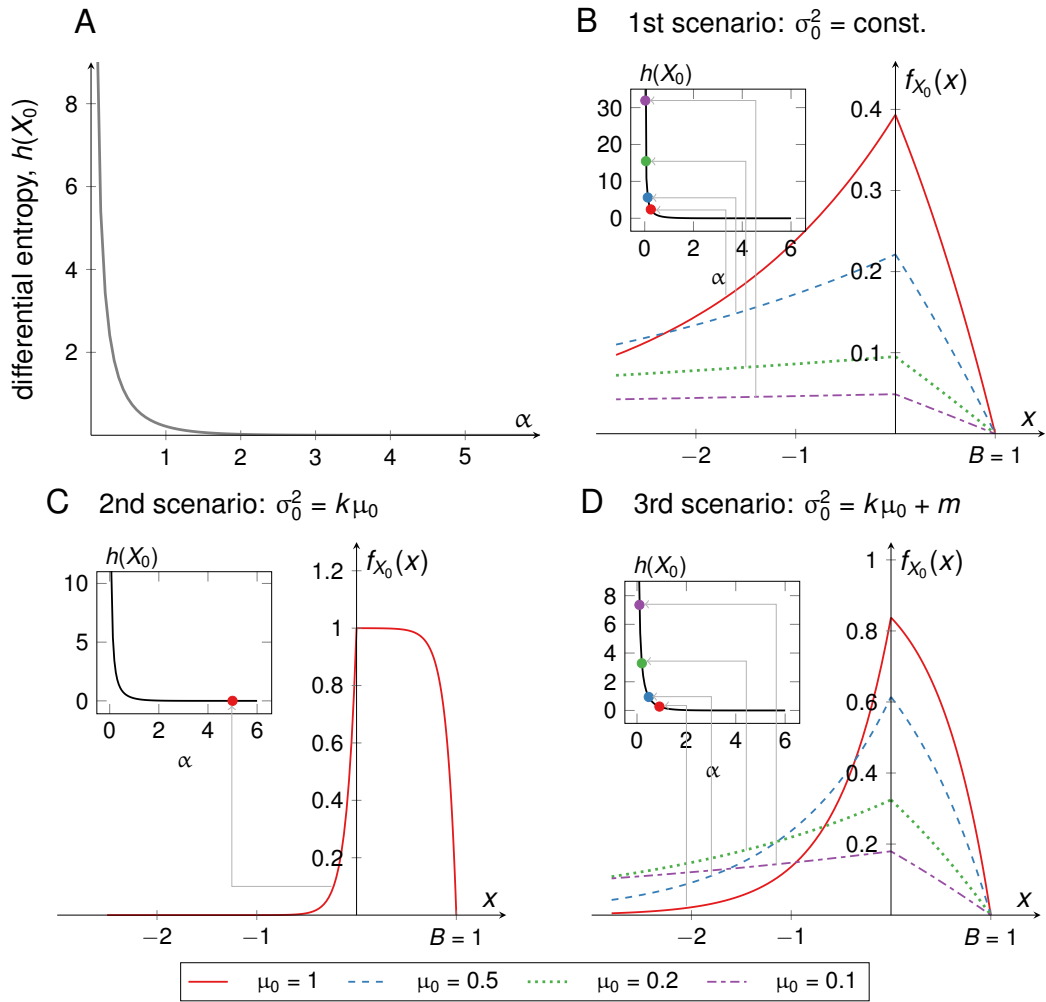
Figure 4: Influence of μ_0 on the pdf f_{X_0} and on the differential entropy $h(X_0)$ of X_0, the random position of the Wiener process at time of stimulation t_0. Panel A: Differential entropy of X_0 as a function of $\alpha = \mu_0/\sigma_0^2$. Panel B: Pdf of X_0 for the constant diffusion parameter $\sigma_0^2 = 4$. Panel C: Pdf of X_0 for the proportional diffusion parameter $\sigma_0^2 = k\mu_0$ when $k = 0.2$. In this case, neither f_{X_0} nor $h(X_0)$ depend on μ_0. Panel D: Pdf of X_0 for the linearly proportional diffusion parameter $\sigma_0^2 = k\mu_0 + m$ when $k = 0.1$ and $m = 1$. Insets in the upper left corners of panels B, C and D illustrate the differential entropy $h(X_0)$ for the chosen values of μ_0 under the different assumptions for σ_0^2. Note that the differential entropy is lower for those μ_0 yielding peaked f_{X_0}.